

A derivative-based approach for the leading order hadronic contribution to $g_\mu - 2$

Eric B. Gregory*

*Bergische Universität Wuppertal, 42097 Wuppertal, Germany
Jülich Supercomputing Centre, 52428 Jülich, Germany
E-mail: gregory@uni-wuppertal.de*

Craig McNeile

*Plymouth University, PL4 8AA Plymouth, United Kingdom
E-mail: craig.mcneile@plymouth.ac.uk*

We describe a lattice approach to calculating the leading-order hadronic contribution to the anomalous magnetic moment of the muon. We employ lattice momentum derivatives, in both the spatial and temporal directions, to determine the hadronic vacuum polarization scalar at low momenta and construct a smooth, integrable function in this momentum region. The method is tested on one hex-smearred Wilson-quark lattice ensemble with physical pion masses

*The 33rd International Symposium on Lattice Field Theory
14 -18 July 2015
Kobe International Conference Center, Kobe, Japan**

*Speaker.

1. Introduction

The calculation of the anomalous magnetic moment of the muon $a_\mu = \frac{(g_\mu - 2)}{2}$ is an important challenge, because a precise theoretical calculation from the standard model of particle physics, which differs from the experimental value, would be an indication of physics beyond the Standard Model. Indeed there is a current tension between the experimental estimate for a_μ , and the value predicted by the standard model. The hadronic contribution to a_μ is the dominant source of uncertainty. There are new experiments at FNAL [1] and J-PARC which plan to reduce the experimental error on a_μ , thus motivating reducing the errors on the theoretical calculation.

In this work we report on the determination of the hadronic vacuum polarization (HVP) contribution to a_μ , using a derivative based method. The lattice determination of $a_\mu^{\text{HVP,LO}}$ was pioneered by Blum [2]. Izubuchi [3] has reviewed recent developments in calculating $a_\mu^{\text{HVP,LO}}$ using lattice QCD.

The strategy used in this, and most previous lattice QCD calculations, is as follows. First vector current correlators are used to calculate the hadronic vacuum polarization (HVP) tensor in momentum space:

$$\Pi_{\mu\nu}(\hat{q}) = \sum_x e^{iq(\Delta x + \frac{a\hat{0}}{2})} \langle J_\mu^{\text{CVC}}(x_0) J_\nu^{\text{loc}}(x) \rangle. \quad (1.1)$$

Here J_ν^{loc} is the local vector current and J_μ^{CVC} is the lattice conserved vector current which satisfies the Ward identity for the modified momentum $\hat{q}_\mu = \frac{2}{a} \sin(\frac{aq_\mu}{2})$. From this one determines a HVP scalar

$$\Pi(s) \equiv \Pi_{\mu\nu}(\hat{q}) / T_{\mu\nu}(\hat{q}), \quad (1.2)$$

with the momentum tensor $T_{\mu\nu}(\hat{q}) \equiv (\hat{q}_\mu \hat{q}_\nu - \hat{q}^2 \delta_{\mu\nu})$, and $s = q^2$

The lowest-order contribution to a_μ^{had} is given by

$$a_\mu^{\text{had,LO}} = \frac{\alpha}{\pi} \int_0^\infty ds f(s) \Pi(s), \quad (1.3)$$

using the kernel function

$$f(s) = \frac{m_\mu^2 s Z(s)^3 (1 - sZ(s))}{1 + m_\mu^2 s Z(s)^2}, \quad \text{where } Z = -\frac{s - \sqrt{s^2 + 4m_\mu^2 s}}{2m_\mu^2 s}. \quad (1.4)$$

In general only values of $\Pi(s)$ are known at discrete lattice momenta, so some procedure is needed to determine a smooth function $\Pi(s)$. In the past some groups have relied upon fitting a function, such as a vector meson dominance model, to the lattice values of $\Pi(s)$. This model-dependence introduces potentially significant systematic effects [4]. A further challenge is that one cannot directly access the zero-momentum value of $\Pi(s)$ through equation 1.2. This makes it harder to constrain the low-momentum values which contribute the most to the integral in equation 1.3.

We propose a moments-based method that addresses each of these concerns. We determine spatial and temporal momentum derivatives of $T_{\mu\nu}(\hat{q})$. To estimate the spatial derivatives requires additional correlators to be measured. From these momentum derivatives we can calculate the corresponding derivatives of the HVP scalar $\Pi(s)$. We use Taylor expansions to interpolate $\Pi(s)$ to non-lattice values of s . Our method produces a model-independent smooth curve for $\Pi(s)$ and

allows direct access to the zero-momentum value of $\Pi(s)$. This produces a high-precision determination of $\Pi(s)$ in the crucial low-momentum region of the integrand of (1.3). De Rafael [5] has shown that $a_\mu^{\text{had,LO}}$ can be reconstructed from up to three derivatives of $\Pi_p(s)$.

2. Outline of the method

We begin by determining the HVP vector and the its first N derivatives with respect to momenta q_{α_i} for $i = 1, \dots, N$:

$$\Pi_{\mu\nu}(\hat{q}) = \sum_x e^{iq(\Delta x + \frac{a\hat{t}}{2})} \langle J_\mu^{\text{CVC}}(x_0) J_\nu^{\text{loc}}(x) \rangle \quad (2.1)$$

$$\frac{\partial^n \Pi_{\mu\nu}(\hat{q})}{\partial q_{\alpha_1} \cdots \partial q_{\alpha_n}} = i^n \sum_x \left[\prod_\rho \left(\Delta x_{\alpha_\rho} + \frac{\delta_{\mu\alpha_\rho}}{2} \right) \right] e^{iQ(\Delta x + \frac{a\hat{t}}{2})} \langle J_\mu^{\text{CVC}}(x_0) J_\nu^{\text{loc}}(x) \rangle. \quad (2.2)$$

We generally determine $N = 8$ derivatives of $\Pi_{\mu\nu}$ using both spatial and temporal moments, which we will see gives three derivatives of $\Pi(s)$. Other groups, e.g. [6], have used temporal moments. However apart from the proposal in [7], no other groups, to our knowledge, have taken advantage of the spatial moments.

First we transform derivatives of $\Pi_{\mu\nu}$ with respect to q , to derivatives with respect to \hat{q} . This is straightforward with the chain rule. To determine derivatives of $\Pi(s)$ we again apply the chain rule. Linear expressions relate derivatives of $\Pi(s)$ and $\Pi_{\mu\nu}(q)$:

$$\frac{\partial^n \Pi_{\mu\nu}}{\partial q_{\alpha_1} \cdots \partial q_{\alpha_n}}(q) = \sum_{m=0}^n A_{\mu\nu}^{\{\alpha\}^n}_m(q) \frac{d^m \Pi(s)}{ds^m}. \quad (2.3)$$

The superscript $\{\alpha\}$ is shorthand for the set of indices $\alpha_1 \cdots \alpha_n$. We will occasionally suppress the $\{\alpha\}$ for readability. Recursion expressions relate the A_m^n to $A_{\mu\nu 0}^0(q) = T_{\mu\nu}(q)$. The $m = 0$ terms are derivatives of $T_{\mu\nu}(q)$:

$$\begin{aligned} A_{\mu\nu 0}^{\{\alpha\}^n}(q) &= \partial_{\alpha_n} \cdots \partial_{\alpha_1} A_{\mu\nu 0}^0(q) \\ &= \partial_{\alpha_n} \cdots \partial_{\alpha_1} T_{\mu\nu}(q). \end{aligned} \quad (2.4)$$

Note that $T_{\mu\nu}(q)$ has only three non-zero derivatives:

$$A_{\mu\nu 0}^{\{\alpha\}^n}(q) = \begin{cases} T_{\mu\nu}(q) &= q_\mu q_n u - q^2 \delta_{\mu\nu} & \text{for } n = 0 \\ \frac{\partial T_{\mu\nu}}{\partial q_{\alpha_1}} &= \delta_{\mu\alpha_1} q_\nu + \delta_{\nu\alpha_1} q_\mu - 2\delta_{\mu\nu} q_{\alpha_1} & \text{for } n = 1 \\ \frac{\partial^2 T_{\mu\nu}}{\partial q_{\alpha_1} \partial q_{\alpha_2}} &= \delta_{\mu\alpha_1} \delta_{\nu\alpha_2} + \delta_{\mu\alpha_2} \delta_{\nu\alpha_1} + 2\delta_{\mu\nu} \delta_{\alpha_1\alpha_2} & \text{for } n = 2 \\ \frac{\partial^n T_{\mu\nu}}{\partial q_{\alpha_1} \cdots \partial q_{\alpha_n}} &= 0 & \text{for } n < 2 \end{cases} \quad (2.5)$$

One finds also that the when $m = n$

$$A_{\mu\nu n}^{\{\alpha\}^n}(q) = \begin{cases} 2q_{\alpha_n} A_{\mu\nu n-1}^{\{\alpha\}^{n-1}} & \text{for } n < 3 \\ 0 & \text{for } n \geq 3, \end{cases} \quad (2.6)$$

and, in general

$$A_{\mu\nu m}^{\{\alpha\}^n} = 2q_{\alpha_n} A_{\mu\nu m-1}^{\{\alpha\}^{n-1}} + \partial_{q_{\alpha_n}} A_{\mu\nu m}^{\{\alpha\}^{n-1}}. \quad (2.7)$$

The expressions for $A_{\mu\nu m}^{\{\alpha\}^n}$ tend to have a large number of terms. We have a script that generates algebraic and C code expressions for these.

For non-zero momentum we can now compute $\frac{\partial^n \Pi_{\mu\nu}(\hat{q})}{\partial q_{\alpha_1} \cdots \partial q_{\alpha_n}}$ by solving the linear system (2.3).

For $s = 0$ we must be slightly more savvy. The factors of q in $A_{\mu\nu m}^{\{\alpha\}^n}$ cause unwanted divergences. Coefficients $A_{\mu\nu m}^{\{\alpha\}^n}(q)$ have $(2 - n) + 2m$ powers of momentum. So for any value of m , needed to find the m^{th} derivative of $\Pi(s)$, $n = 2 + 2m$ gives a constant coefficient with no q -dependence. Then we can solve

$$\left. \frac{d^m \Pi}{ds^m} \right|_{s=0} = \frac{1}{A_{\mu\nu m}^{\{\alpha\}^{(2+2m)}}} \left. \frac{\partial^{(2+2m)} \Pi_{\mu\nu}}{\partial \hat{q}_{\alpha_1} \cdots \partial \hat{q}_{\alpha_{2+2m}}} \right|_{\hat{q}=0}. \quad (2.8)$$

We concern ourselves with the first three derivatives of $\Pi(s)$. So at $s = 0$ the relevant coefficients are $A_{\mu\nu 0}^2$, $A_{\mu\nu 2}^4$, $A_{\mu\nu 1}^6$, and $A_{\mu\nu 3}^8$. What remains is to find the cases where the A_m^n are constant for $n = m + 2$. For these cases the constants are combinations of Kronecker deltas. To make the most of our data we attempt to classify these contributing index combinations. For $n = 2$, $m = 0$ we have two cases

$$A_{\mu\nu 0}^{\{\alpha\}^2} = (\delta_{\alpha_1 \mu} \delta_{\alpha_2 \nu} - 2\delta_{\mu\nu} \delta_{\alpha_1 \alpha_2}) = \begin{cases} -2 & \text{for } \mu = \nu, \alpha_1 = \alpha_2, \alpha_1 \neq \mu \\ 1 & \text{for } \mu = \alpha_1, \nu = \alpha_2, \mu \neq \nu \end{cases} \quad (2.9)$$

In Tab. 1 we summarize the A_0^2 . We label the label diagonal in μ and ν as the ‘‘A20d0’’ channel. There are $N_{\text{comb}} = 12$ index combinations that contribute. If we explore all the possible index values for the off-diagonal $\mu \neq \nu$ case, which we label ‘‘A20od0’’, there are $N_{\text{comb}} = 24$ contributions. However α_1 and α_2 are interchangeable, so the number of independent second derivatives of $\Pi_{\mu\nu}$ that contribute is smaller. We use a local source at the sink and a conserved vector current (CVC) source at the sink, so μ and ν are distinguishable. We therefore have $N_{cl} = 12$ combinations for ‘‘A20od0’’. Had we used CVC at both ends we would have only $N_{cc} = 6$ combinations. We see that in total for our local-CVC setup, we have 24 independent measurements of $\frac{\partial^2 \Pi_{\mu\nu}(0)}{\partial \hat{q}_{\alpha_1} \partial \hat{q}_{\alpha_2}}$ which contribute to our estimate of $\Pi(s = 0)$. The contributing index channels for A_0^2 are summarized graphically in Fig. 1. We classify the contributing channels for A_1^4 , A_2^6 , and A_3^8 in Figs. 2, 3 and 4, respectively. The numbers of contributing independent index configurations for each channel of A_0^2 , A_1^4 , A_2^6 , and A_3^8 are summarized in Tab. 1

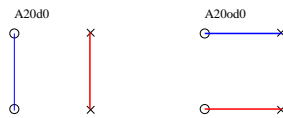


Figure 1: Graphical depiction of contributing A_0^2 index combinations. Circles represent the μ and ν indices, crosses represent α indices. Colored bars indicate the connected indices have the same value.

2.1 Smooth curve generation

For s between two lattice momenta $s_i < s < s_{i+1}$, we make ‘‘lower’’ and ‘‘upper’’ estimates,

$$\Pi^{\text{low}}(s) = \sum_n (s - s_i)^n \frac{1}{n!} \left. \frac{d^n \Pi}{ds^n} \right|_{s_i} \quad \text{and} \quad \Pi^{\text{up}}(s) = \sum_n (s - s_{i+1})^n \frac{1}{n!} \left. \frac{d^n \Pi}{ds^n} \right|_{s_{i+1}} \quad (2.10)$$

A_0^2	label	N_{comb}	N_{cl}	N_{cc}
-2	A20d0	12	12	12
1	A20od0	24	12	6
total		36	24	18

A_1^4	label	N_{comb}	N_{cl}	N_{cc}
-24	A41d0	12	12	12
-8	A41d1	72	12	12
-4	A41d2	72	12	12
<hr/>				
+2	A41od0	288	24	12
+6	A41od1	96	24	12
total		540	84	60

A_2^6	label	N_{comb}	N_{cl}	N_{cc}
-360	A62d0	12	12	12
-72	A62d1	360	24	24
-48	A62d2	180	12	12
-24	A62d3	180	12	12
-24	A62d3a	360	4	4
-16	A62d4	1080	12	12
<hr/>				
+4	A62od0	2160	12	6
+12	A62od1	3600	48	24
+36	A62od2	240	12	6
+60	A62od3	144	24	12
total		8316	172	124

A_2^6	label	N_{comb}	N_{cl}	N_{cc}
-6720	A83d0	12	12	12
-960	A83d1	672	24	24
-720	A83d2	336	12	12
-576	A83d3	840	12	12
-288	A83d4	840	12	12
-240	A83d5	336	12	12
-192	A83d6	5040	12	12
-144	A83d7	10080	12	12
-96	A83d8	5040	12	12
-48	A83d9	10080	4	4
<hr/>				
+24	A83od0	60480	24	12
+72	A83od1	26880	48	24
+120	A83od2	9408	48	24
+360	A83od3	1344	24	12
+840	A83od4	192	24	12
total		131580	292	208

Table 1: Combinations contributing to non-zero A_0^2 , A_0^2 , A_0^2 and A_0^2 .

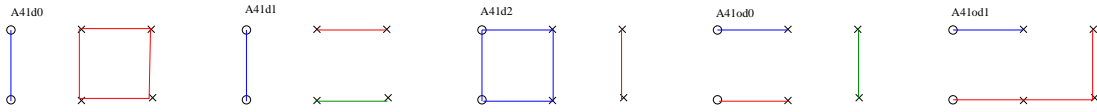


Figure 2: Graphical depiction of contributing A_1^4 index combinations.

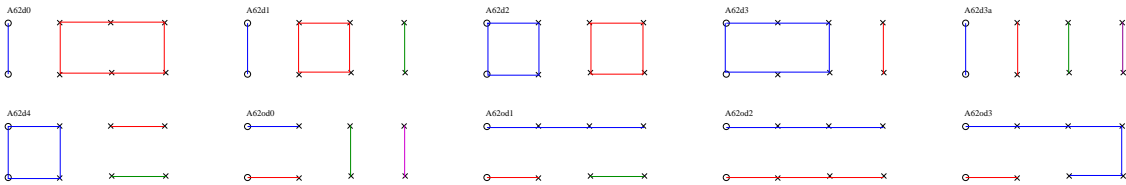


Figure 3: Graphical depiction of contributing A_2^6 index combinations.

We combine these in a weighted average to get a smooth function Π^{sm} for the integrand of (1.3).

$$\Pi_p^{\text{sm}}(s) = \frac{\Pi^{\text{low}}(s)w^{\text{low}}(s) + \Pi^{\text{up}}(s)w^{\text{up}}(s)}{w^{\text{low}}(s) + w^{\text{up}}(s)} \quad (2.11)$$

with

$$w^{\text{low}}(s) = \frac{1}{\left| (s - s_i) \sigma \left(\frac{d\Pi}{ds} \Big|_{s_i} \right) \right|^p} \quad \text{and} \quad w^{\text{up}}(s) = \frac{1}{\left| (s - s_{i+1}) \sigma \left(\frac{d\Pi}{ds} \Big|_{s_{i+1}} \right) \right|^p}. \quad (2.12)$$

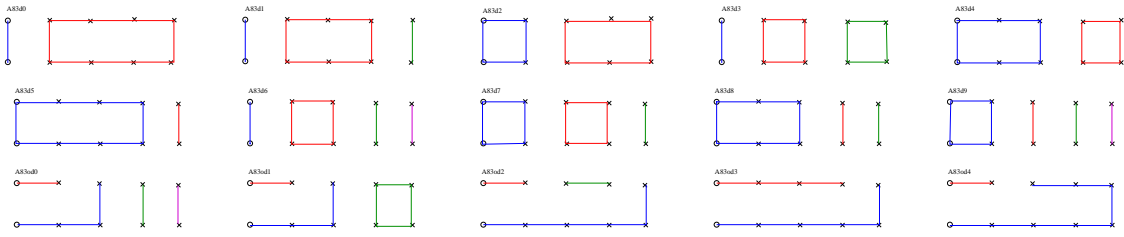


Figure 4: Graphical depiction of contributing A_3^8 index combinations.

$\sigma\left(\frac{d\Pi}{ds}\right)$ is a proxy for the uncertainty in $\Pi^{\text{low/up}}$ and p is an adjustable parameter.

3. Numerical tests

We have tested this method on several of the $N_f = 2 + 1$ flavor 2-HEX ensembles from BMW-c [8]. For this work we concentrate on the ensemble listed in Tab. 2, which has the advantage of having 1060 configurations and $L_s = L_t$. The strange quark mass is mis-tuned on this ensemble, so the data from the additional ensembles is needed to correct for it. We show in Fig. 5 that the different channels for each A_m^n yield consistent estimates of $\frac{d^m\Pi}{ds^m}$. In Fig. 6 we test different methods of computing a smooth function of Π , including different values of p . We note as a curiosity, the large error that would be induced by neglecting the $s = 0$ point, and how well one might do using *only* the $s = 0$ point. Fig. 7 demonstrates that $n = 3$ is a sufficient expansion order for determining a smooth function Π .

a_{ud}^{bare}	a_s^{bare}	volume	# cfgs	M_π (GeV)
-0.05294	-0.0060	$\beta = 3.5, a^{-1} = 2.131$ GeV	1060	0.130(2)
$64^3 \times 64$				

Table 2: Configuration parameters.

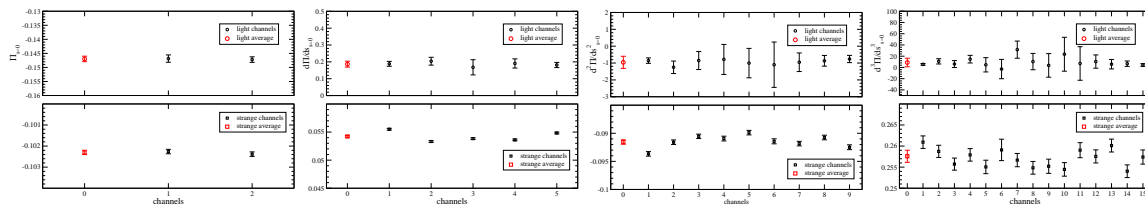


Figure 5: Test of consistency of estimates of $\frac{d^m\Pi}{ds^m}$ from different channels.

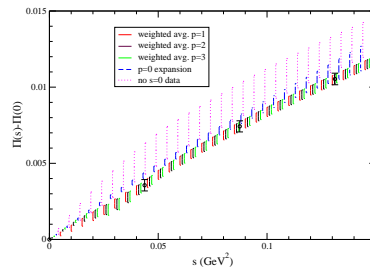


Figure 6: Smooth $\Pi(s)$ curves generated with different values of p .

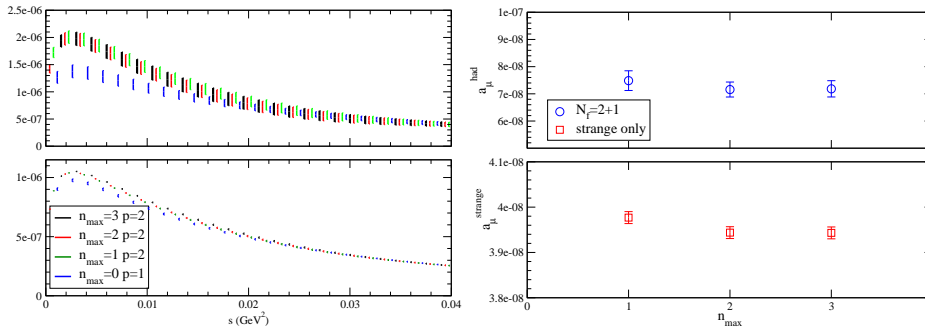


Figure 7: The dependence on the maximum expansion order n of the integrand (l) and a_{HVP} (r).

4. Conclusions

The method described above uses many estimates of the spatial and temporal moments to make a precise determination of $\Pi(s)$ and its derivatives at both finite and zero momentum. Additional systematic errors need to be studied such as finite volume effects [9].

Including spatial as well as temporal moments greatly increases the number of estimates of Π and its derivatives at $s = 0$ one can obtain from each source on each configuration. The $s = 0$ point is the most important in the determination of a_{HVP} , because it is so much closer to the peak of the integrand in equation 1.3, than the first finite s lattice momentum available for current lattice volumes. The most important lattice measurement one can make for determining $a_\mu^{\text{HVP,LO}}$ is $\left. \frac{d\Pi}{ds} \right|_{s=0}$, because $\Pi(0)$ is subtracted off. Our method produces 172 estimates of $\left. \frac{d\Pi}{ds} \right|_{s=0}$ for each source.

The authors thank the Gauss Centre for Supercomputing (GCS) for providing computing time through the John von Neumann Institute for Computing (NIC) on the GCS share of the supercomputer JUQUEEN at Jülich Supercomputing Centre (JSC) and time granted on JUROPA at JSC. This work used the DiRAC Blue Gene Q Shared Petaflop system at the University of Edinburgh, operated by the Edinburgh Parallel Computing Centre on behalf of the STFC DiRAC HPC Facility (www.dirac.ac.uk).

References

- [1] Muon $g-2$, J. Grange *et al.*, (2015), arXiv:1501.06858.
- [2] T. Blum, Phys. Rev. Lett. **91**, 052001 (2003), arXiv:hep-lat/0212018.
- [3] T. Izubuchi, Lattice qcd moments - $g - 2$ and nedm , 2015, Talk presented at the lattice 2015 conference.
- [4] M. Golterman, K. Maltman, and S. Peris, Phys. Rev. **D90**, 074508 (2014), arXiv:1405.2389.
- [5] E. de Rafael, Phys. Lett. **B736**, 522 (2014), arXiv:1406.4671.
- [6] HPQCD, B. Chakraborty *et al.*, Phys. Rev. **D89**, 114501 (2014), arXiv:1403.1778.
- [7] G. M. de Divitiis, R. Petronzio, and N. Tantalo, Phys. Lett. **B718**, 589 (2013), arXiv:1208.5914.
- [8] S. Durr *et al.*, Science **322**, 1224 (2008), arXiv:0906.3599.
- [9] Budapest-Marseille-Wuppertal, R. Malak *et al.*, PoS **LATTICE2014**, 161 (2015), arXiv:1502.02172.